Submitted to the Journal of Biomechanical Engineering – October 2021 (GCMB-2021-0291.R1)

Evaluating Stability of Human Spine in Static Tasks: A Combined *In Vivo*-Computational Study

F. Ghezelbash[1]; A. Shahvarpour[2]; C. Larivière[2]; A. Shirazi-Adl[1]

[1] Division of Applied Mechanics, Department of Mechanical Engineering, Polytechnique Montréal, Canada

[2] Institut de recherche Robert Sauvé en santé et en sécurité du travail, Montréal, Canada

Abstract word count: 198

Manuscript word count: ~4160

Corresponding Author:

Farshid Ghezelbash

Division of Applied Mechanics, Polytechnique Montreal, Canada, H3C 3A7

Email: ghezelbash.far@gmail.com

Abstract

Various interpretations and parameters have been proposed to assess spinal stability such as antagonist muscle coactivity, trunk stiffness and spinal buckling load; however, the correlation between these parameters remains unknown. We evaluated spinal stability during different tasks while changing the external moment and load height and investigated likely relationships between different EMG- and model-based parameters (e.g., EMG coactivity ratio, trunk stiffness, force coactivity ratio) and stability margins. EMG and kinematics of 40 young healthy subjects were recorded during various quasi-static tasks. Muscle forces, trunk stiffness and stability margins were calculated by a nonlinear subject-specific EMG-assisted-optimization musculoskeletal model of the trunk. The load elevation and external moment increased muscle activities and trunk stiffness while all stability margins (i.e., buckling loads) decreased. The force coactivity ratio was strongly correlated with the hand-load stability margin (i.e., additional weight in hands to initiate instability; R^2=0.54) demonstrating the stabilizing role of abdominal muscles. The total trunk stiffness (Pearson's r=0.96) and the sum of EMGs of back muscles (Pearson's r=0.65) contributed the most to the T1 stability margin (i.e., additional required load at T1 for instability/buckling). Force coactivity ratio and trunk stiffness can be used as alternative spinal stability metrics.

Keywords: Spine Biomechanics; Spinal Stability; Musculoskeletal Modeling; Finite Element Modeling

1 Introduction

The ligamentous lumbar spine alone (without muscles) buckles even under small compressive loads; ~80 N (Crisco III and Panjabi 1992; Crisco et al. 1992) while during daily activities, the entire spine undergoes large compression forces, frequently exceeding 3000 N (Ghezelbash, Shirazi-Adl, El Ouaaid, et al. 2020; Ghezelbash, Shirazi-Adl, Plamondon, et al. 2020), with no instability. Such a discrepancy between in vitro and in vivo observations highlights the stabilizing role of muscles, as active components (Panjabi 1992). Despite numerous definitions for and interpretations of a system stability that exist in the literature, the complex neuro-musculoskeletal human spine is qualified to be stable as long as its responses (e.g., relative displacements of vertebrae) remain small and bounded under small perturbations. Instability, in both clinical and biomechanical contexts, can be interpreted as hypermobility, e.g., excessive intersegmental laxity which can impair the normal function of spine and cause injury and pain (Panjabi 2003; Reeves et al. 2007, 2011). Some studies have employed the stability concept to develop clinical exercises (Vezina and Hubley-Kozey 2000; McGill and Karpowicz 2009); however, the accurate quantification of the spinal stability remains as a major concern (Oxland 2016). Due to the difficulty in measurements, different mathematical methods have been proposed to quantify spinal stability (Bergmark 1989; El-Rich et al. 2004; Shirazi-Adl et al. 2005; Granata and England 2006; Asgari et al. 2015). Though employing similar definitions, these methods distinctively quantify the spinal stability (Graham and Brown 2012). Among existing methods, musculoskeletal biomechanical models have been employed to estimate muscle forces as well as the spinal stability during dynamic (Bazrgari et al. 2009; Shahvarpour et al. 2015) or static (El Ouaaid et al. 2013; Shamsi et al. 2017; Sharifi et al. 2017) tasks using kinematics-driven optimization (Ghezelbash et al. 2015), EMG-assisted-optimization (Cholewicki and McGill 1994; Gagnon et al. 2016, 2018) or EMG-driven (Brown and McGill 2010; Graham and Brown 2012) methods.

With regard to the stability, biomechanical models determine the margin of safety (or stability margin) as the additional load that the system can support while remaining stable. If the magnitude of the additional load or applied perturbation exceeds the stability margin, the spine ceases to be stable. In upright standing, subjects holding loads at constant lever arms and hence under nearly constant external moments, Granata and Orishimo (2001) measured higher activity in the surface EMG of abdominal as well as extensor muscles with the load elevation. Using a single degree of freedom model with two muscle groups, they argued that such increases in muscle activity are due to the trunk stability demand, which deteriorates at higher load elevations. The trunk stability has also been found dependent on other parameters such as the trunk stiffness, force/EMG coactivity ratio, and magnitude of the external loads (Gardner-Morse et al. 1995; van Dieën, Cholewicki, et al. 2003; Potvin and Brown 2005a; Rashedi et al. 2010; El Ouaaid et al. 2013). In those studies, however, a correlation between foregoing parameters and spinal stability has been assumed. For example, spinal stiffness is interchangeably used with spinal stability (van Dieën, Kingma, et al. 2003; El

Ouaaid et al. 2013; Reeves et al. 2019; van den Hoorn et al. 2020), but the exact correlation between foregoing parameters and spinal stability at different external moments and load elevations has not been established.

In order to address these issues, we aimed to (1) evaluate the spinal stability during multiple tasks while changing the external moment and load height and (2) to investigate the likely relationship between different EMG- and model-based parameters (e.g., EMG coactivity ratio, trunk stiffness, force coactivity ratio) as well as stability margins using both in vivo measurements and a subject-specific EMG-assisted-optimization musculoskeletal model of the trunk. After collecting EMG and trunk kinematics during different static tasks (three positions and three hand-load magnitudes), we calculated different EMG/model-based parameters such as coactivity ratios, muscle forces and stability margins. Correlation and regression analyses were performed to explore and identify possible relationships between foregoing parameters. We hypothesized that changes in the external moment and load height significantly affect stability margins as well as EMG- and model-based parameters.

2 Methods

2.1 Experiments

A brief description of methods is provided here as a detailed description is available elsewhere (Larivière et al. 2019). After an approval by the institutional ethics committee and signing a consent form, each of the 40 young healthy subjects (20 females and 20 males; Table 1) performed various sagittal-symmetric weight-holding tasks at an upright standing posture. Participants held three weights (0%, 5% and 10% of body weight) at three positions in both hands (Fig. 1). In the first and second tasks, loads were held at an identical moment arm to the L5-S1 disc (L_0=12% of the subject body height, Fig. 1) but at two different heights (L5-S1 and shoulder levels, Fig. 1). In the third task, the moment arm of the external load was increased as the load was held at an extended arm position in front at the shoulder joint height, Fig. 1c. Rotations in the sagittal plane along the spine (C7, T11 and S1) were recorded at 100 Hz using inertial sensors (Xsens Technologies, Netherlands), Supplementary Materials 2. Measured signals were low-pass filtered by a zero-lag fourth-order Butterworth filter (corner frequency of 3 Hz). Activity of superficial muscles (longissimus at T11 and L1, Iliocostalis, multifidus, external oblique, internal oblique and rectus abdominis) were collected at 1000 Hz using 14 surface electromyography (EMG) electrodes (Delsys Inc., MA, USA) (for electrode locations see (Larivière et al. 2001; Shahvarpour et al. 2017)). To reduce the noise, filtered signals were band-pass filtered (30-450 Hz; 8th order zero-lag Butterworth IRR filter) (Redfern et al. 1993), and after full-wave rectification, fourth-order zero-lag low-pass filter was used to obtain EMG amplitudes. EMG signals were normalized to their corresponding maximum EMG amplitude recorded during maximum voluntary isometric contractions in flexion, extension, lateral and axial directions. Each task was repeated twice, and average values of normalized EMGs and rotations were taken as model inputs and for subsequent statistical analyses.

2.2 Musculoskeletal Modeling

Equilibrium analysis: To evaluate muscle forces, spinal loads and stability margin, we used our nonlinear subject-specific finite element musculoskeletal model. The model incorporated nonlinear moment-rotation and force-displacement properties of the passive spine (by equivalent shear-deformable beams for each of T11-S1 motion segments representing disc, facet joints and ligaments; and beams were offset posteriorly by 2 mm from the disc geometric center (Ghezelbash, Eskandari, et al. 2018)) along with 126 sagittally symmetric muscles (Ghezelbash, Eskandari, et al. 2018). To individualize the muscle architecture in our musculoskeletal model, we scaled muscle moment arms and physiological cross-sectional areas by using image-based regression equations (Anderson et al. 2012) with body weight, body height, sex and age as independent variables. For the passive mechanical properties, on the other hand, disc cross-sectional area and height at different levels were scaled based on available datasets (Shi et al. 2014) and proportional to the body height (Ghezelbash et al. 2016), respectively (Fig. S1 – Supplementary Materials 1). Euler's beam theory was employed when modifying passive joint properties (i.e., force-strain and moment-curvature) in accordance with subject's body height, body weight, sex and age (Fig. S1 – Supplementary Materials 1). Segmental masses at different spinal levels as well as arms and head were adjusted proportional to the subject's body weight (Ghezelbash et al. 2016; Ghezelbash et al. 2017). Trunk kinematics (T11 and S1 rotations) as well as muscle activities were personalized based on kinematic as well as electromyography measurements in each task. Further details about the model scaling are available in (Ghezelbash et al. 2016).

In the kinematics-driven approach, we prescribed T11 and S1 rotations in the nonlinear finite element model based on our in vivo measurements (Supplementary Materials 2). In addition, intersegmental rotations in between these two levels (T12 to L5) were applied assuming 6.0%, 10.9%, 14.1%, 13.2%, 16.9%, 20.1% and 18.7% proportions of the total T11-S1 rotation from the cranial T11-T12 to the caudal L5-S1 levels (Ghezelbash et al. 2016). Computed reaction moments at each level were counterbalanced by muscle forces that were estimated from an EMG-assisted optimization algorithm, Fig. S3. Muscle forces were initially computed from EMG measurements:

$$F = \sigma_{max} \,.\, PCSA \,.\, nEMG, \qquad \text{Eq. 1}$$

where F represents muscle force, and σ_{max} denotes maximum muscle stress (varied among muscles groups; see Table 3 in (Ghezelbash, El Ouaaid, et al. 2018)), $PCSA$ is the physiological cross sectional area (Stokes and Gardner-Morse 1999; Anderson et al. 2012), and $nEMG$ is the normalized EMG. While satisfying the moment equations of equilibrium at each level, foregoing initial muscle forces were modified by a correction factor, g (Fig. S3 – Supplementary Materials):

$$F = g.\sigma_{max} \,.\, PCSA \,.\, nEMG, \qquad \text{Eq. 2}$$

in which g was sought for each muscle through an optimization framework (Cholewicki and McGill 1994; Gagnon et al. 2018), Fig. S3:

$$\min_{g_i} \sum_i M_i(1-g_i)^2. \quad \text{Eq. 3}$$

M_i is the muscle moment estimated for the i^{th} muscle (Gagnon et al. 2018). Muscle forces were constrained to be positive and smaller than the maximum allowable limit ($0 < F < \sigma_{max}\,.PCSA$) (Ghezelbash, El Ouaaid, et al. 2018). Estimated muscle forces were applied as external loads onto corresponding vertebrae and then iteratively updated. The equilibrium analysis was repeated until convergence (<1% changes in muscle forces between two successive iterations); Fig. S3 – Supplementary Materials 1. We assumed that EMG activities of deeper iliopsoas and quadratus lumborum muscles were the same as those of internal oblique and longissimus (at L1), respectively (Cholewicki and McGill 1996; Gagnon et al. 2016).

Stability analysis: To estimate the spinal stability at each task and after the evaluation of muscle forces as described above, muscles were replaced with linear springs:

$$k = \frac{qF}{l}, \quad \text{Eq. 4}$$

where k, q, F and l denote the instantaneous muscle stiffness, a non-dimensional constant, current muscle force and muscle length (Bergmark 1989; Cholewicki and McGill 1994). After replacing muscles with pre-loaded springs (carrying forces estimated earlier in the EMG-assisted optimization approach), all rotational boundary conditions (except at S1) were removed, which is necessary when performing stability analyses. Therefore and unlike the equilibrium analysis, prescribed rotations were not considered in the stability analyses and the external loads along with pre-loaded springs (representing muscles) deformed the spine to its final configuration (the same as in vivo measurements used to drive the model in the prior equilibrium analysis). The agreement between the final computed configuration and measured vertebral rotations further demonstrated that equilibrium equations were correctly computed and enforced in the EMG-assisted optimization approach. A linear buckling analysis was performed to estimate stability margins (i.e., buckling load or reserve load). In linear buckling analysis after applying preloads (hand-load, gravity forces and muscle forces), a perturbation load should be chosen, and the buckling analysis estimates the magnitude of this perturbation load which causes instability. In structural mechanics, the perturbation load is often known because of design considerations. In spine biomechanics, however, the location of the perturbation load is arbitrary. We performed the linear buckling analysis by placing the perturbation load at two different locations (hands and T1; Fig. 1), and define two stability margins (or buckling loads) for the system (q=70 in all muscles). The hand-load stability margin shows the additional hand-load needed before the instability while T1 stability margin is the load required at the T1 for spinal instability.

2.3 Parameters

In addition to load height and external load moment, we defined various EMG- and model-based parameters to explore their likely associations with the spinal stability:

- **Back and abdominal muscles activities:**

$$\text{Back Muscles Activity} = \sum \text{nEMGs of Back Muscles}$$
$$\text{Abdominal Muscles Activity} = \sum \text{nEMGs of Abdominal Muscles} \quad \text{Eq. 5}$$

- **EMG coactivity ratio:** This represents the ratio of antagonist EMG activity in all 3 abdominal muscles relative to all:

$$\text{EMG Coactivity} = \frac{\sum \text{nEMGs of Abdominal Muscles}}{\sum \text{nEMGs of All Muscles}} \quad \text{Eq. 6}$$

- **Force coactivity ratio:** This ratio was computed similar to EMG coactivity ratio, but with forces taken from the subject-specific finite element model at the T11 level alone (i.e., global abdominal and extensor thoracic muscles).
- **Trunk stiffness:** Differentiating muscle moments at the S1 with respect to the trunk (T11) rotational degree of freedom in the sagittal plane (θ) yields trunk angular stiffness (Rashedi et al. 2010; Pfeifer et al. 2012):

$$\frac{\partial M}{\partial \theta} = \frac{\partial}{\partial \theta}\left(\sum_i F_i r_i\right) = \sum_i \left(r_i \frac{\partial F_i}{\partial l_i}\frac{\partial l_i}{\partial \theta} + \frac{\partial r_i}{\partial \theta} F_i\right), \quad \text{Eq. 7}$$

where M, θ and r are net moment generated by muscles, trunk inclination in the sagittal plane and muscle moment arm in the sagittal plane, respectively. Using Eq. 4 and $r_i = \frac{\partial l_i}{\partial \theta}$, Eq. 7 is expanded as follows:

$$\text{Trunk Stiffness} = \overbrace{\sum_i q\frac{F_i r_i^2}{l_i}}^{1^{\text{st}}\ \text{Trunk Stiffness}} + \overbrace{\sum_i \frac{\partial^2 l_i}{\partial \theta^2} F_i}^{2^{\text{nd}}\ \text{Trunk Stiffness}}, \quad \text{Eq. 8}$$

in which q was set at 5, and F was estimated from the musculoskeletal model.

- **T1 stability margin:** Load to be applied at the T1 for the trunk instability (Fig. 1). For details, see Stability Analysis section.
- **Hand-load stability margin:** Additional hand-load required for the trunk instability (Fig. 1). For details, see Stability Analysis section.

2.4 Statistical Analysis

To identify likely relationships among influential variables, we used multivariate regression and correlation analyses. To avoid multicollinearity in the regression analysis, Belsley's test was used (Belsley et al. 2005), and among

predictors with correlation coefficient > 0.8, the one yielding the largest coefficient of determination in regression analysis was chosen.

3 Results

Females had greater (though non-significant) nEMG sum of abdominal and back muscles (Table 2; Figs 2 and 3). The external moment significantly increased nEMG sum of abdominal (p-value<0.001) and back muscles (p-value<0.001) while load elevation significantly increased the activation in back muscles but not in abdominals (Table 2; Figs 2 and 3). In both EMG- and model-based parameters, load elevation and external moment decreased EMG and force coactivity ratios of abdominal muscles (Figs 2 and 3) while increasing trunk stiffness (Table 3).

Females in average had greater spinal stability (Figs 2 and 3). Force coactivity significantly influenced stability measures (Table 4), and force coactivity alone was the strongest predictor of hand-load stability margin (Fig. 4a and Table 5). The trunk stiffness substantially contributed to all stability measures (Table 4) and particularly to the T1 stability margin, Fig. 4 and Table 5. Increasing the external moment and load elevation reduced hand-load stability margin (Figs 2 and 3, and Table 2). Back muscles activity and abdominal muscles activity significantly affected the T1 stability spinal margin (Table 4). Force coactivity and model second trunk stiffness ($\sum_i \frac{\partial^2 l_i}{\partial \theta^2} F_i$; Eq. 8) alone explained 54% and 40% of the variance in hand-load stability margin (Fig. 4a and b). Although both hand-load and T1 stability margins quantify spinal stability, they were weakly correlated (Pearson's r=0.35; Table 5).

4 Discussion

In this study, we aimed to investigate alterations in muscle recruitment strategy and spinal stability measures when changing load elevation and external moment. The external moment decreased EMG coactivity ratio despite increases in the abdominal muscle activities. Load elevation and external moment increased muscle activities and trunk stiffness, yet the hand-load stability margin decreased. The force coactivity ratio was strongly associated with the hand-load stability margin (R^2=0.54; Fig. 4a) while the trunk stiffness was the major contributing factor to the T1 stability margin (R^2=0.93; Fig. 4c). Hand-load and T1 stability margins were weakly correlated (Pearson's r=0.35) and hence should not be taken as equivalent measures of spinal stability.

4.1 Limitations

In this study and in accordance with the stated objectives, we only considered static tasks; the extension of these results to transient conditions require additional experimental works. Notwithstanding a complex nonlinear relationship between the EMG and force (particularly in presence of smaller muscle activities) (Solomonow et al. 1991; Buchanan et al. 2004; Brown and McGill 2008), we assumed a linear relationship (Eq. 1). The surface EMG records

activities in superficial muscles close to electrodes while we neglected cross-talks and assumed identical activity in all portions of larger and deeper muscles. Muscle force estimations are sensitive to σ_{max} (Eq. 1) (Mohammadi et al. 2015), but because σ_{max} was assumed identical among subjects, the relative difference in computed stability measures between subjects was not affected. Measurements and muscle modeling confirm that the muscle stiffness is proportional to its force (similar to Eq. 4), but the stiffness-length relation is likely more complex (Cholewicki and McGill 1995), and Bergmark's relation (Eq. 4) may lose accuracy in transient conditions with varying muscle length; however, since all tasks were performed at erect standing posture with negligible changes in muscle lengths, the use of Bergmark's relation likely remain valid in this study. For the same reason, muscle passive forces were overlooked. The proposed trunk stiffness (Eq. 8) only represented the global stiffness (about L5-S1) and overlooked intersegment stiffnesses. Still, it was a strong predictor of T1 stability margin (R^2>90%). In the majority of tasks, the critical q (at which the stability margin reaches zero) remained below 50. q=70 was considered to reach convergence in most simulations and to make a meaningful comparison between tasks. It should be noted that based on in vitro experiments, q varies between 0.5 and 170 (Cholewicki and McGill 1995), and q=70 is within the physiological range. To individualize the musculoskeletal model, we used mechanical principles and dimensional analysis in conjunction with existing regression equations; therefore, some variations between the scaled models and participants in our study (e.g., differences in PCSA) likely existed. However, in the view of the relative accuracy of used datasets (Anderson et al. 2012; Shi et al. 2014) and equilibrium equations as constraints, these variations are not expected to affect our conclusions. The scaling algorithm adjusted passive properties of the ligamentous spine by using the beam theory (Fig. S1 – Supplementary Materials 1), which yielded satisfactory results in comparison with detailed finite element results, as shown in Fig. S2 – Supplementary Materials 1 (Natarajan and Andersson 1999). While considering changes in the crucial parameters such as the disc height and area, this method did not incorporate likely individual variations in other components (e.g., facet joints and ligaments). It is to be noted that all simulated tasks were at the erect standing posture in which the effect of passive responses was relatively small.

4.2 Interpretations

External moment was positively proportional to the activity of back and abdominal muscles (Table 2). Agonist (back) muscles were activated to counterbalance the external moment while the activity of antagonist (abdominal) muscles might be attributed to improve spinal stability. At identical external moment, load elevation (Figs 1a and b) did not significantly affect abdominal activities although it increased back muscles activities (Table 2). Granata and Orishimo (2001) found that activity in abdominal muscles (the average of external oblique and rectus abdominis) significantly increased with the load elevation. They, however, compared the average of external oblique and rectus while we used the sum of activities in all abdominal muscles. In corroboration with (Granata and Orishimo 2001), the load height increased, though not as much, the EMG activity in back muscles (p-value<0.001). In our study, the EMG

coactivity ratio decreased significantly with the load elevation and external moment (Table 2; Figs 2 and 3) that could be due to the relative increases in the activity of back muscles compared to abdominals. Females had greater abdominal muscle activities and therefore greater stability margins, which may be due to the larger activation of external oblique in females (Larivière et al. 2019). Besides, lower body weight and hence axial compression on the spine can also play a stabilizing role in females.

The notion that abdominal coactivation (or contraction) and trunk stiffness are correlated with the spinal stability is a popular concept (van Dieën, Kingma, et al. 2003; Madinei et al. 2018; Reeves et al. 2019; Mehrez and Smaoui 2020; van den Hoorn et al. 2020). However, apart from few studies using a single joint model (Brown and McGill 2005; Potvin and Brown 2005b), no study has comprehensively established such a relationship. Our results demonstrated that only T1 stability margin was strongly correlated with the trunk stiffness (Pearson's r = 0.62; Table 5) while abdominal coactivation alone was weakly correlated with the T1 stability margin (Pearson's r = 0.17; Table 5); therefore, the foregoing notion (though popular) is not strictly accurate. Our earlier studies on the stability of the knee joint in gait (Sharifi et al. 2017) and the spine in upright standing (El Ouaaid et al. 2013) clearly demonstrated that antagonist coactivity can stabilize the joints only when acting at a lower intensity levels while high coactivation levels can even deteriorate the stability.

We defined two sets of stability measures by estimating buckling load (additional load required for instability) at hands and at the T1. The physical interpretation of the hand-load stability margin is straightforward: How much additional load can one carry in hands, for a given posture and muscles activity, until instability occurs. However, the T1 stability margin considers the application of load at the T1 until buckling. These two stability margins were however weakly correlated (Pearson's r ~0.35; Table 5); this demonstrates that the system stability margin depends on where the perturbation load is applied. In the model, the T1 to T11 is considered as a single rigid body, and performing buckling analysis at the T1 or T11 yields the same trend although at different magnitudes, so the T1 stability margin may infer the core stability index, which is strongly associated with the trunk stiffness (Tables 4 and 5).

The force coactivity ratio significantly affected both stability margins, Table 4 (van Dieën, Cholewicki, et al. 2003), and it was positively associated with the hand-load stability margin (Table 4) but not with the T1 stability margin (Table 4). The external moment and force coactivity ratio were found inversely proportional (Table 2), which shows that the relative changes in the activities of abdominal muscles over back muscles decreased under larger external moments. Greater abdominal coactivity ratio not only stabilized the spine but also increased spinal loads (Tables 4 and 5); therefore, the foregoing inverse relation appears beneficial in maintaining stability. It should be noted that different abdominal coactivity indices have been proposed (Le et al. 2017). Those indices, which are correlated with Eq. (Ranavolo et al. 2015), might also be correlated with the hand-load stability margin.

Trunk stiffness and its components (particularly the 2nd trunk stiffness = $\sum_i \frac{\partial^2 l_i}{\partial \theta^2} F_i$) significantly influenced stability margins. The trunk stiffness (1st trunk stiffness and total trunk stiffness) alone could explain ~92% of the variation in the T1 stability margin (Fig. 4 and Table 5) whereas the 2nd trunk stiffness explained nearly 40% of variation in the hand-load stability margin (Fig. 4). This suggests a viable alternative approach to cumbersome stability analyses; one can estimate spinal stability margin quite accurately without performing buckling analyses by estimating trunk stiffness and force coactivity ratio. Additionally, force coactivity ratio was strongly correlated with the 2nd trunk stiffness (Pearson's r=0.80; Table 5) but not the total trunk stiffness (Pearson's r=0.33; Table 5), so greater coactivity ratio improves only the hand-load stability margin but not the T1 stability margin.

A linear relation exists between the trunk stiffness and stability index (or margin) in a simplified 2D inverted pendulum with a single degree of freedom:

$$\text{Stability Index} = \overbrace{\sum_i F_i \left(q \frac{r_i^2}{l_i} + \frac{d^2 l_i}{d\theta^2}\right)}^{\text{Trunk Stiffness}} + k_{spine} - W_g \frac{d^2 h_g}{d\theta^2} - W_{ext} \frac{d^2 h_{ext}}{d\theta^2} \qquad \text{Eq. 9}$$

where k_{spine} denotes the angular stiffness of the passive ligamentous spine, and W_g (W_{ext}) and h_g (h_{ext}) are the gravity (external) load and height, respectively. This simple analytical example demonstrates how the trunk angular stiffness is related to the stability index. It should be noted that Granata and Orishimo (2001) neglected the $\sum_i \frac{d^2 l_i}{\partial \theta^2} F_i$ term. Also, the definition of the trunk stiffness used in this study (Eq. 8) is different from others taken in system identification approaches (Cholewicki et al. 2000; Hodges et al. 2009; Hendershot et al. 2011; Shojaei et al. 2018).

5 Conclusions

We evaluated the spinal stability for various static tasks when the external moment and load height were altered. Likely relationships between different EMG/model parameters (e.g., trunk stiffness, force coactivity ratio) and stability margins were investigated using our subject-specific finite element EMG-assisted-optimization musculoskeletal model of the trunk. In average, females showed higher spinal stability than males. The load elevation and external moment increased muscle activities and trunk stiffness, yet all stability margins decreased. The force coactivity ratio was strongly associated with the hand-load stability margin (i.e., additional hand-load to initiate instability; R^2=0.54), which demonstrated the stabilizing role of abdominal muscles. The trunk stiffness as well as the sum of nEMGs of back and abdominal muscles contributed the most to the T1 stability margin (i.e., additional required load at T1 for instability). The hand-load stability margin and T1 stability margin were two distinct stability measures when quantifying the trunk stability. Some parameters calculated from the measured EMG (back and abdominal muscles activity) or from a

musculoskeletal model (force coactivity ratio, total trunk stiffness and second trunk stiffness) can be employed to estimate the trunk hand-load stability without performing stability analyses.

6 Acknowledgement

Ali Shahvarpour had a post doctoral scholarship from the Institut de recherche Robert-Sauvé en santé et en sécurité du travail (IRSST) of Quebec, Canada. The authors would like to thank Christina Gravel, Myriam Gauvin, Anne-Marie Jean, Ariane Viau and Cynthia Appleby for data collection, Hakim Mecheri for data processing, as well as Dr. Amir Hossein Eskandari for his comments and helps. This work was supported by the institut de recherche Robert-Sauvé en santé et en sécurité du travail (IRSST-2019-0018), fonds de recherche du Québec en nature et technologies (FRQNT-200564) and Mitacs (IT18289).

7 References

Anderson DE, D'Agostino JM, Bruno AG, Manoharan RK, Bouxsein ML. 2012. Regressions for estimating muscle parameters in the thoracic and lumbar trunk for use in musculoskeletal modeling. J Biomech. 45(1):66-75.

Asgari M, Sanjari MA, Mokhtarinia HR, Sedeh SM, Khalaf K, Parnianpour M. 2015. The effects of movement speed on kinematic variability and dynamic stability of the trunk in healthy individuals and low back pain patients. Clin Biomech. 30(7):682-688.

Bazrgari B, Shirazi-Adl A, Lariviere C. 2009. Trunk response analysis under sudden forward perturbations using a kinematics-driven model. J Biomech. 42(9):1193-1200.

Belsley DA, Kuh E, Welsch RE. 2005. Regression diagnostics: Identifying influential data and sources of collinearity. Vol. 571. John Wiley & Sons.

Bergmark A. 1989. Stability of the lumbar spine: a study in mechanical engineering. Acta Orth Scand. 60(sup230):1-54.

Brown SH, McGill SM. 2005. Muscle force–stiffness characteristics influence joint stability: a spine example. Clin Biomech. 20(9):917-922.

Brown SH, McGill SM. 2008. Co-activation alters the linear versus non-linear impression of the EMG–torque relationship of trunk muscles. J Biomech. 41(3):491-497.

Brown SH, McGill SM. 2010. The relationship between trunk muscle activation and trunk stiffness: examining a non-constant stiffness gain. Comput Method Biomec. 13(6):829-835.

Buchanan TS, Lloyd DG, Manal K, Besier TF. 2004. Neuromusculoskeletal modeling: estimation of muscle forces and joint moments and movements from measurements of neural command. J App Biomech. 20(4):367-395.

Cholewicki J, McGill SM. 1994. EMG assisted optimization: a hybrid approach for estimating muscle forces in an indeterminate biomechanical model. J Biomech. 27(10):1287-1289.

Cholewicki J, McGill SM. 1995. Relationship between muscle force and stiffness in the whole mammalian muscle: a simulation study. J Biomech Eng. 117(3):339-342.

Cholewicki J, McGill SM. 1996. Mechanical stability of the in vivo lumbar spine: implications for injury and chronic low back pain. Clin Biomech. 11(1):1-15.

Cholewicki J, Simons AP, Radebold A. 2000. Effects of external trunk loads on lumbar spine stability. J Biomech. 33(11):1377-1385.

Crisco III J, Panjabi M. 1992. Euler stability of the human ligamentous lumbar spine. Part I: Theory. Clin Biomech. 7(1):19-26.

Crisco J, Panjabi M, Yamamoto I, Oxland T. 1992. Euler stability of the human ligamentous lumbar spine. Part II: Experiment. Clin Biomech. 7(1):27-32.

El-Rich M, Shirazi-Adl A, Arjmand N. 2004. Muscle activity, internal loads, and stability of the human spine in standing postures: combined model and in vivo studies. Spine. 29(23):2633-2642.

El Ouaaid Z, Shirazi-Adl A, Arjmand N, Plamondon A. 2013. Coupled objective function to study the role of abdominal muscle forces in lifting using the kinematics-driven model. Comput Methods Biomech Biomed Eng. 16(1):54-65.

Gagnon D, Plamondon A, Larivière C. 2016. A biomechanical comparison between expert and novice manual materials handlers using a multi-joint EMG-assisted optimization musculoskeletal model of the lumbar spine. J Biomech. 49(13):2938-2945.

Gagnon D, Plamondon A, Larivière C. 2018. A comparison of lumbar spine and muscle loading between male and female workers during box transfers. J Biomech. 81:76-85.

Gardner-Morse M, Stokes IA, Laible JP. 1995. Role of muscles in lumbar spine stability in maximum extension efforts. J Orthop Res. 13(5):802-808.

Ghezelbash F, Arjmand N, Shirazi-Adl A. 2015. Effect of intervertebral translational flexibilities on estimations of trunk muscle forces, kinematics, loads, and stability. Comput Method Biomec. 18(16):1760-1767.

Ghezelbash F, El Ouaaid Z, Shirazi-Adl A, Plamondon A, Arjmand N. 2018. Trunk musculoskeletal response in maximum voluntary exertions: A combined measurement-modeling investigation. J Biomech. 70:124-133.

Ghezelbash F, Eskandari A, Shirazi-Adl A, Arjmand N, El-Ouaaid Z, Plamondon A. 2018. Effects of motion segment simulation and joint positioning on spinal loads in trunk musculoskeletal models. J Biomech. 70:149-156.

Ghezelbash F, Shirazi-Adl A, Arjmand N, El-Ouaaid Z, Plamondon A. 2016. Subject-specific biomechanics of trunk: musculoskeletal scaling, internal loads and intradiscal pressure estimation. Biomech Model Mechanobiol. 15(6):1699-1712.

Ghezelbash F, Shirazi-Adl A, El Ouaaid Z, Plamondon A, Arjmand N. 2020. Subject-specific regression equations to estimate lower spinal loads during symmetric and asymmetric static lifting. J Biomech. 102:109550.

Ghezelbash F, Shirazi-Adl A, Plamondon A, Arjmand N. 2020. Comparison of different lifting analysis tools in estimating lower spinal loads–Evaluation of NIOSH criterion. J Biomech. 112:110024.

Ghezelbash F, Shirazi-Adl A, Plamondon A, Arjmand N, Parnianpour M. 2017. Obesity and Obesity Shape Markedly Influence Spine Biomechanics: A Subject-Specific Risk Assessment Model. Ann Biomed Eng.

Graham RB, Brown SH. 2012. A direct comparison of spine rotational stiffness and dynamic spine stability during repetitive lifting tasks. J Biomech. 45(9):1593-1600.

Granata KP, England SA. 2006. Stability of dynamic trunk movement. Spine. 31(10):E271.

Granata KP, Orishimo KF. 2001. Response of trunk muscle coactivation to changes in spinal stability. J Biomech. 34(9):1117-1123.

Hendershot B, Bazrgari B, Muslim K, Toosizadeh N, Nussbaum MA, Madigan ML. 2011. Disturbance and recovery of trunk stiffness and reflexive muscle responses following prolonged trunk flexion: influences of flexion angle and duration. Clin Biomech. 26(3):250-256.

Hodges P, van den Hoorn W, Dawson A, Cholewicki J. 2009. Changes in the mechanical properties of the trunk in low back pain may be associated with recurrence. J Biomech. 42(1):61-66.

Larivière C, Gagnon D, Gravel D, Arsenault AB, Dumas J-P, Goyette M, Loisel P. 2001. A triaxial dynamometer to monitor lateral bending and axial rotation moments during static trunk extension efforts. Clin Biomech. 16(1):80-83.

Larivière C, Shahvarpour A, Gravel C, Gauvin M, Jean A-M, Viau A, Mecheri H. 2019. Revisiting the effect of manipulating lumbar stability with load magnitudes and positions: the effect of sex on trunk muscle activation. J Electromy Kines.

Le P, Aurand A, Dufour JS, Knapik GG, Best TM, Khan SN, Mendel E, Marras WS. 2017. Development and testing of a moment-based coactivation index to assess complex dynamic tasks for the lumbar spine. Clin Biomech. 46:23-32.

Madinei S, Motabar H, Ning XJE. 2018. The influence of external load configuration on trunk biomechanics and spinal loading during sudden loading. 61(10):1364-1373.

McGill SM, Karpowicz AJAopm. 2009. Exercises for spine stabilization: motion/motor patterns, stability progressions, and clinical technique. Arch Phys Med Rehabil. 90(1):118-126.

Mehrez S, Smaoui H. 2020. Directional Dependence of Experimental Trunk Stiffness: Role of Muscle-Stiffness Variation of Nonneural Origin. Appl Bionics Biomech. 2020.

Mohammadi Y, Arjmand N, Shirazi-Adl A. 2015. Comparison of trunk muscle forces, spinal loads and stability estimated by one stability-and three EMG-assisted optimization approaches. Med Eng Phys. 37(8):792-800.

Natarajan RN, Andersson GB. 1999. The influence of lumbar disc height and cross-sectional area on the mechanical response of the disc to physiologic loading. Spine. 24(18):1873.

Oxland TR. 2016. Fundamental biomechanics of the spine—What we have learned in the past 25 years and future directions. J Biomech. 49(6):817-832.

Panjabi MM. 1992. The stabilizing system of the spine. Part I. Function, dysfunction, adaptation, and enhancement. J Spinal Disord. 5:383-383.

Panjabi MM. 2003. Clinical spinal instability and low back pain. J Electromy Kines. 13(4):371-379.

Pfeifer S, Vallery H, Hardegger M, Riener R, Perreault EJ. 2012. Model-based estimation of knee stiffness. IEEE Transactions on Biomedical Engineering. 59(9):2604-2612.

Potvin JR, Brown SH. 2005a. An equation to calculate individual muscle contributions to joint stability. Journal of Biomechanics. 38(5):973-980.

Potvin JR, Brown SH. 2005b. An equation to calculate individual muscle contributions to joint stability. J Biomech. 38(5):973-980.

Ranavolo A, Mari S, Conte C, Serrao M, Silvetti A, Iavicoli S, Draicchio F. 2015. A new muscle co-activation index for biomechanical load evaluation in work activities. Ergonomics. 58(6):966-979.

Rashedi E, Khalaf K, Nassajian MR, Nasseroleslami B, Parnianpour M. 2010. How does the central nervous system address the kinetic redundancy in the lumbar spine? Three-dimensional isometric exertions with 18 Hill-model-based muscle fascicles at the L4—L5 level. Proc Inst Mech Eng H. 224(3):487-501.

Redfern MS, Hughes RE, Chaffin DB. 1993. High-pass filtering to remove electrocardiographic interference from torso EMG recordings. Clin Biomech. 8(1):44-48.

Reeves NP, Cholewicki J, Van Dieën JH, Kawchuk G, Hodges PW. 2019. Are stability and instability relevant concepts for back pain? J Orthop Sports Phys Ther. 49(6):415-424.

Reeves NP, Narendra KS, Cholewicki J. 2007. Spine stability: the six blind men and the elephant. Clin Biomech. 22(3):266-274.

Reeves NP, Narendra KS, Cholewicki J. 2011. Spine stability: lessons from balancing a stick. Clin Biomech. 26(4):325-330.

Shahvarpour A, Henry SM, Preuss R, Mecheri H, Larivière C. 2017. The effect of an 8-week stabilization exercise program on the lumbopelvic rhythm and flexion-relaxation phenomenon. Clinical Biomechanics. 48:1-8.

Shahvarpour A, Shirazi-Adl A, Larivière C, Bazrgari B. 2015. Trunk active response and spinal forces in sudden forward loading–analysis of the role of perturbation load and pre-perturbation conditions by a kinematics-driven model. J Biomech. 48(1):44-52.

Shamsi M, Sarrafzadeh J, Jamshidi A, Arjmand N, Ghezelbash F. 2017. Comparison of spinal stability following motor control and general exercises in nonspecific chronic low back pain patients. Clin Biomech. 48:42-48.

Sharifi M, Shirazi-Adl A, Marouane H. 2017. Computational stability of human knee joint at early stance in Gait: Effects of muscle coactivity and anterior cruciate ligament deficiency. J Biomech. 63:110-116.

Shi X, Cao L, Reed MP, Rupp JD, Hoff CN, Hu J. 2014. A statistical human rib cage geometry model accounting for variations by age, sex, stature and body mass index. J Biomech. 47(10):2277-2285.

Shirazi-Adl A, El-Rich M, Pop D, Parnianpour M. 2005. Spinal muscle forces, internal loads and stability in standing under various postures and loads—application of kinematics-based algorithm. Eur Spine J. 14(4):381-392.

Shojaei I, Suri C, van Dieën JH, Bazrgari B. 2018. Alterations in trunk bending stiffness following changes in stability and equilibrium demands of a load holding task. J Biomech. 77:163-170.

Solomonow M, Baratta RV, D'Ambrosia R. 1991. EMG-force relations of a single skeletal muscle acting across a joint: Dependence on joint angle. J Electromy Kines. 1(1):58-67.

Stokes IA, Gardner-Morse M. 1999. Quantitative anatomy of the lumbar musculature. J Biomech. 32(3):311-316.

van den Hoorn W, Cholewicki J, Coppieters MW, Klyne DM, Hodges PW. 2020. Trunk stiffness decreases and trunk damping increases with experimental low back pain. J Biomech. 112:110053.

van Dieën JH, Cholewicki J, Radebold A. 2003. Trunk muscle recruitment patterns in patients with low back pain enhance the stability of the lumbar spine. Spine. 28(8):834-841.

van Dieën JH, Kingma I, Van der Bug J. 2003. Evidence for a role of antagonistic cocontraction in controlling trunk stiffness during lifting. J Biomech. 36(12):1829-1836.

Vezina MJ, Hubley-Kozey CL. 2000. Muscle activation in therapeutic exercises to improve trunk stability. Arch Phys Med Rehabil. 81(10):1370-1379.

Tables

Table 1: Average (standard deviation) of anthropometric measures of participants

Sex	Number of Subjects	Age (year)	Body Weight (kg)	Body Height (cm)	BMI (kg/cm^2)
Females	20	22.95 (2.19)	59.75 (7.33)	1.67 (0.05)	21.49 (2.23)
Males	20	23.20 (2.26)	73.18 (6.21)	1.81 (0.06)	22.36 (1.75)

Table 2: Multivariate regression analysis of EMG-based parameters as well as estimated coefficient, p-value and R^2

Response Variable	Variable	Coefficient	p-value	R^2
Abdominal Muscles Activity	Intercept	16.002	<0.0001	0.167
	Sex*	-3.436	0.0001	
	Load Height	0.004	0.8671	
	External Load Moment	2.528	<0.0001	
Back Muscles Activity	Intercept	-11.755	0.1014	0.629
	Sex*	-11.08	<0.0001	
	Load Height	0.345	<0.0001	
	External Load Moment	17.709	<0.0001	
EMG Coactivity Ratio	Intercept	0.709	<0.0001	0.295
	Sex*	0.008	0.5988	
	Load Height	-0.003	<0.0001	
	External Load Moment	-0.054	<0.0001	

* Female=1; Male=2

Table 3: Multivariate regression analysis of model-based parameters as well as estimated coefficient, p-value and R^2

Response Variable	Variable	Coefficient	p-value	R^2
Force Coactivity	Intercept	31.948	<0.0001	0.386
	Sex*	-0.402	0.6500	
	Load Height	-0.060	0.0144	
	External Load Moment	-5.013	<0.0001	
Trunk Stiffness	Intercept	28.182	0.0006	0.142
	Sex*	-8.931	0.0002	
	Load Height	0.090	0.1430	
	External Load Moment	6.089	<0.0001	

* Female=1; Male=2

Table 4: Multivariate regression analysis of stability measures as well as estimated coefficient, p-value, and R^2

Response Variable	Variable	Coefficient	p-value	R^2
Hand-Load Stability Margin	Intercept	1235.331	<0.0001	0.655
	Sex*	171.313	<0.0001	
	Load Height	-13.267	<0.0001	
	External Load Moment	-56.814	0.0126	
	Force Coactivity	23.280	<0.0001	
	Trunk Stiffness	13.739	<0.0001	
T1 Stability Margin (1st Regression Model Using Model-Based Parameters)	Intercept	188.177	<0.0001	0.951
	Sex*	-24.588	0.0196	
	Load Height	-0.917	0.0023	
	External Load Moment	-10.072	0.1172	
	Force Coactivity	-6.769	<0.0001	
	Trunk Stiffness	21.446	<0.0001	
T1 Stability Margin (2nd Regression Model Using EMG-Based Parameters)	Intercept	602.134	<0.0001	0.679
	Sex*	28.573	0.2798	
	Load Height	-3.577	<0.0001	
	External Load Moment	-173.105	<0.0001	
	EMG Coactivity	-495.951	0.0010	
	Abdominal Muscles Activity	27.938	<0.0001	
	Back Muscles Activity	11.002	<0.0001	

* Female=1; Male=2

Table 5: Correlation matrix of all variables (SM: stability margin; TS: trunk stiffness).

Parameters	Sex	Load Height	External Load Moment	nEMG Sum of Back Muscles	nEMG Sum of Abd. Muscles	Force Coactivity	1st TS	2nd TS	Total TS	Hand-Load SM	T1 SM
Sex											
Load Height	0.33										
External Load Moment	0.17	0.17									
nEMG Sum of Back Muscles	0.03	0.30	0.75								
nEMG Sum of Abd. Muscles	-0.11	0.04	0.34	0.31							
Force Coactivity	-0.17	-0.05	-0.57	-0.32	0.07						
1st TS	-0.03	0.23	0.55	0.73	0.60	0.09					
2nd TS	-0.14	-0.2	-0.78	-0.48	-0.04	0.80	-0.12				
Total TS	-0.08	0.17	0.30	0.57	0.59	0.33	0.95	0.19			
Hand-Load SM	-0.11	-0.35	-0.25	-0.13	0.19	0.62	0.33	0.57	0.50		
T1 SM	-0.07	0.17	0.41	0.65	0.56	0.17	0.96	0.03	0.96	0.35	

Symmetric

Figures

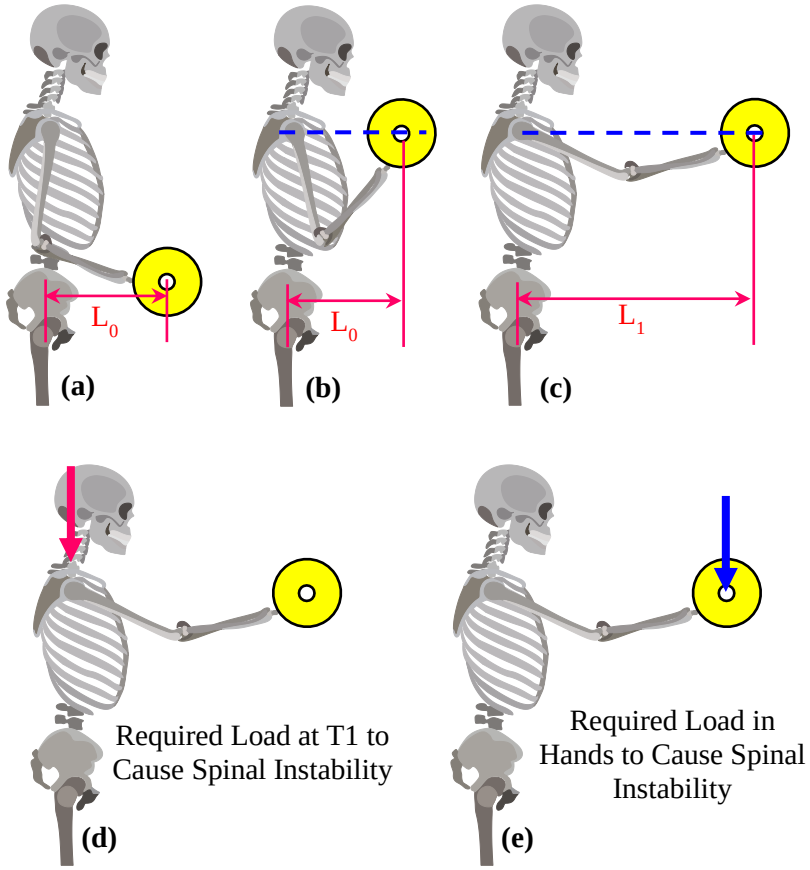

Fig. 1: Schematic representation of performed tasks (a, b, and e), as well as T1 instability margin (d) and hand-load instability margin (e)

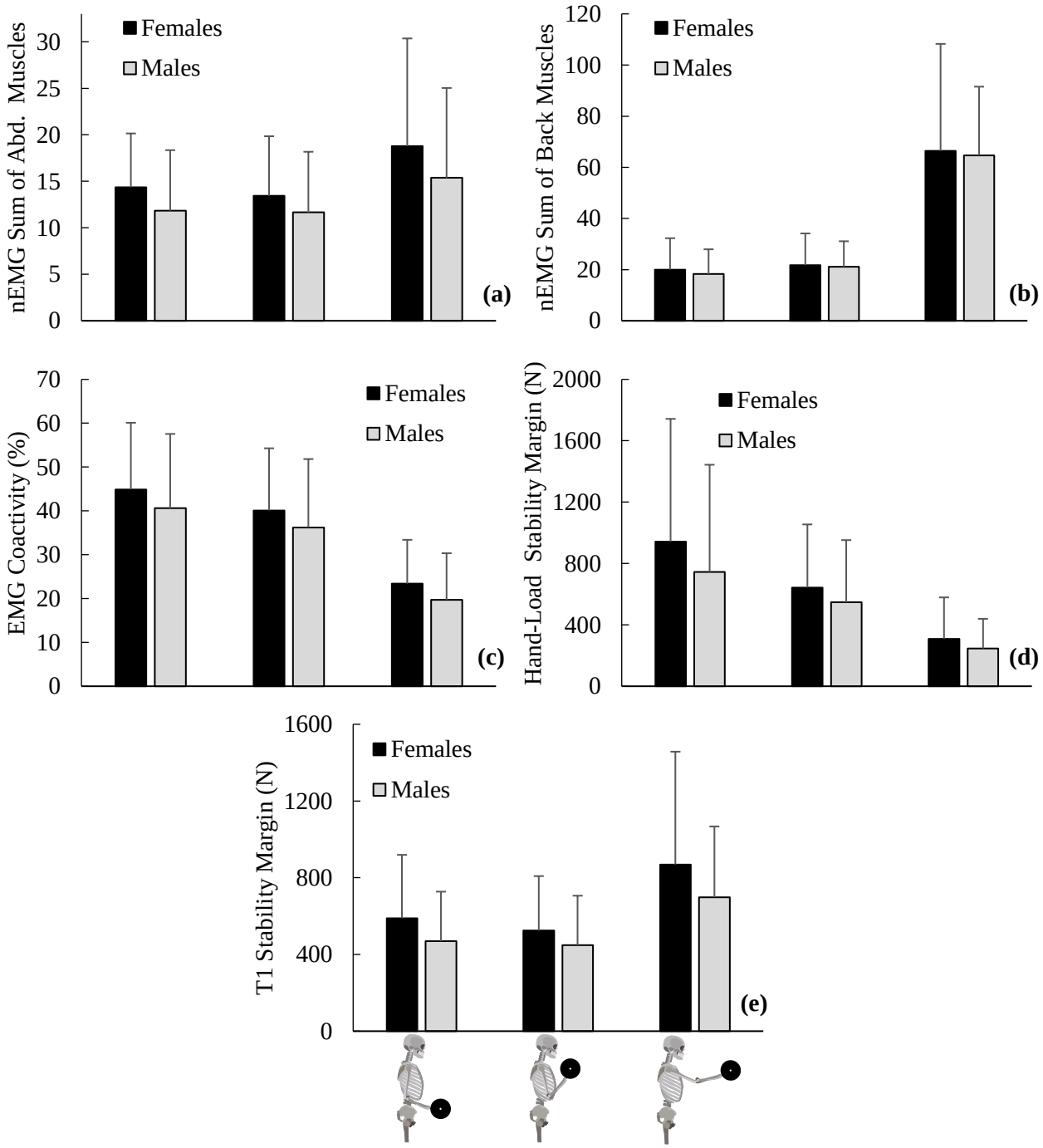

Fig. 2: Average (a) nEMG sum of abdominal muscles, (b) nEMG sum of back muscles, (c) EMG coactivity of abdominal muscles, (d) hand-load stability margin and (e) T1 stability margin in females and males under various tasks and loads

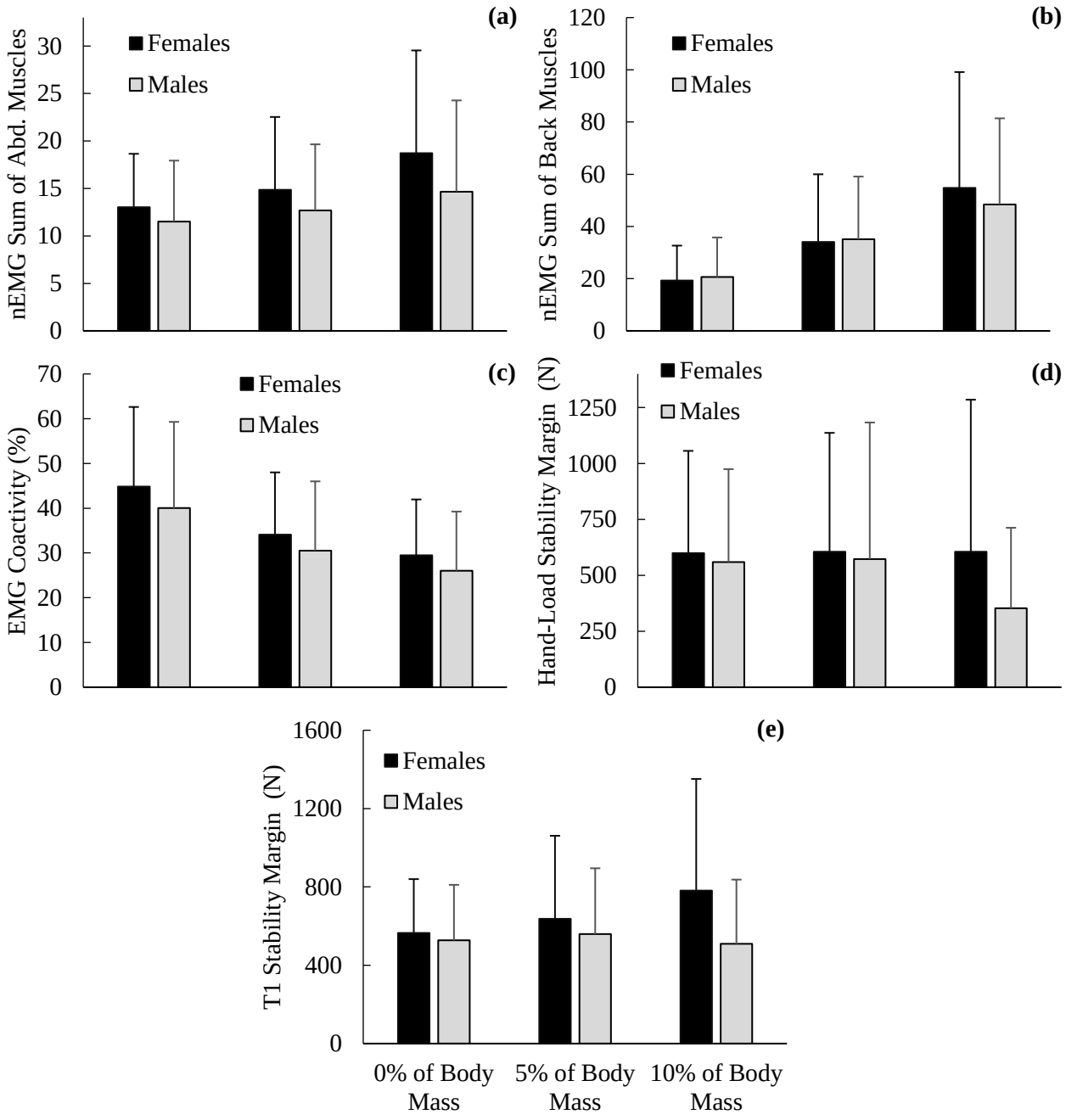

Fig. 3: Average (a) nEMG sum of abdominal muscles, (b) nEMG sum of back muscles, (c) EMG coactivity of abdominal muscles, (d) estimated hand-load stability margin and (e) estimated T1 stability margin in females and males with various hand-loads

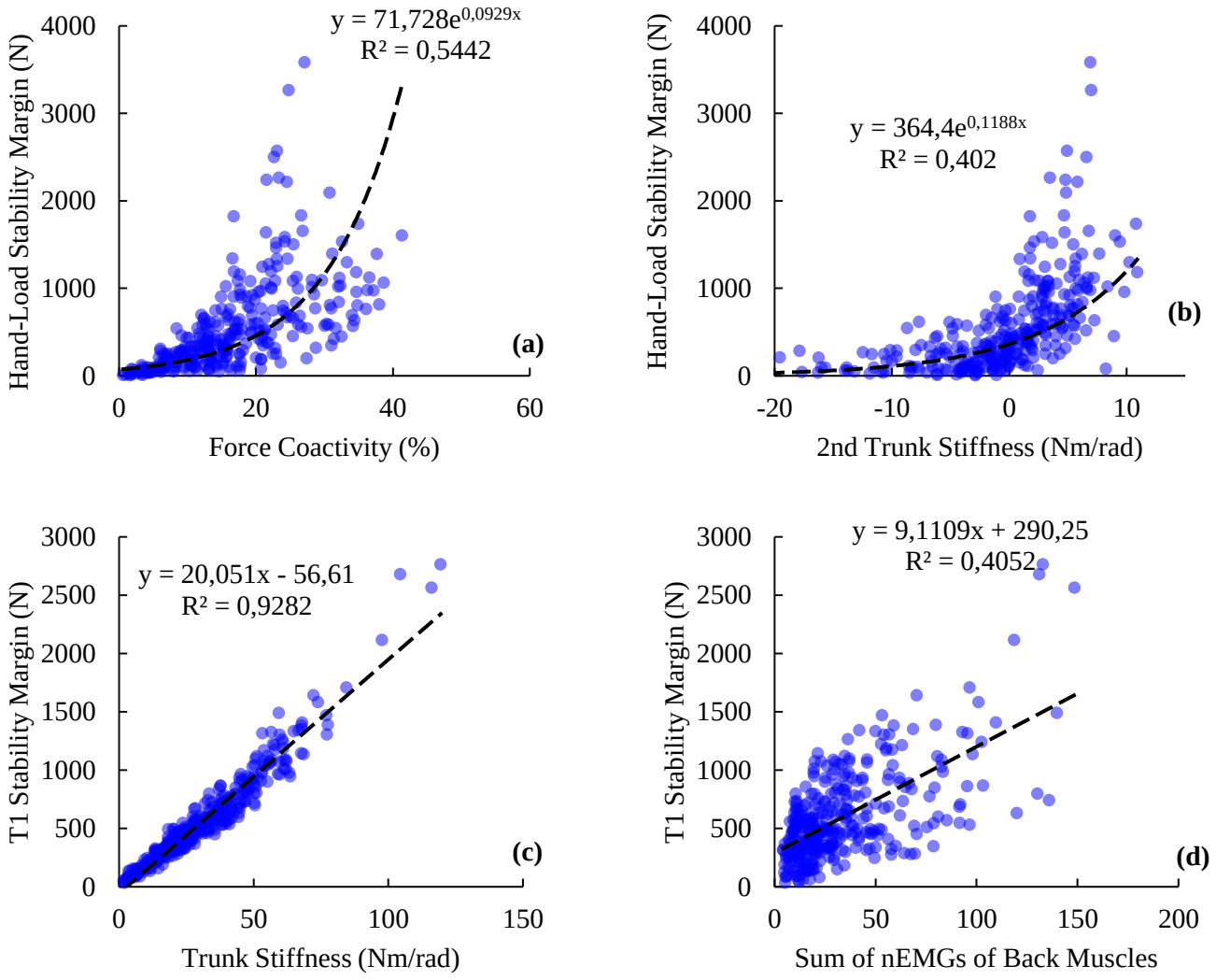

Fig. 4: (a) Force coactivity, (b) 2nd trunk stiffness ($\sum_i \frac{\partial^2 l_i}{\partial \theta^2} F_i$), (c) trunk stiffness and (d) sum of EMGs of back muscles versus stability margin (hand-load and T1) for all subjects and tasks

Supplementary Materials

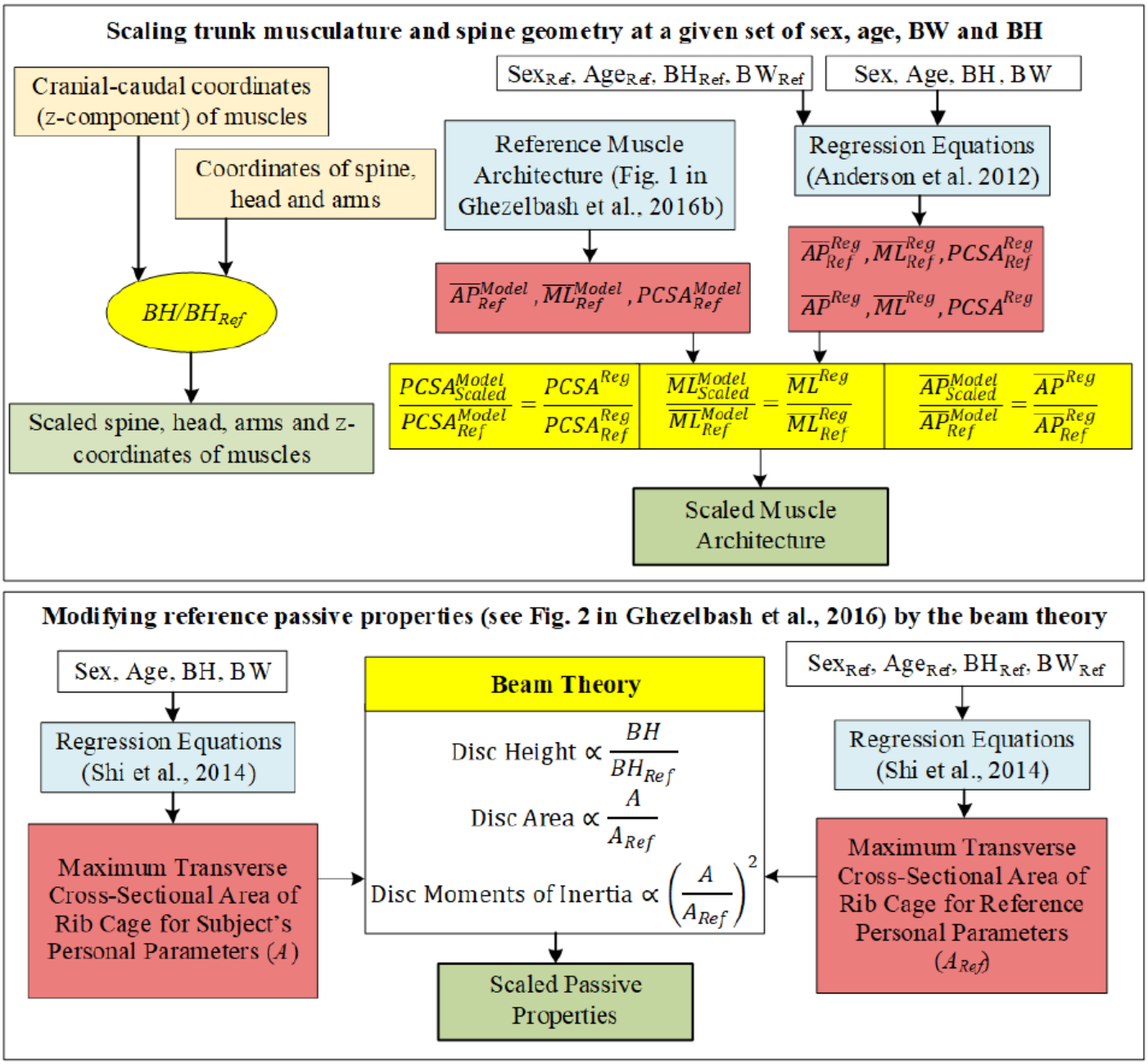

Fig. S1: The flowchart of the scaling algorithm. BH: body height; BW: body weight; PCSA: physiological cross-sectional area; AP: average anterior-posterior distance of a muscle centroid (when cut by a transverse plane) from vertebrae; ML: average medio-lateral distance of a muscle centroid (when cut by a transverse plane) from vertebrae; A: maximum transverse cross-sectional area of the rib cage; "Ref" subscript and "Scaled" superscripts denote reference and personalized values, respectively, and "Reg" superscript represents calculated values from regression equations.

Reference personal parameters: sexref=male, ageref=41.8 year, BHref=173.0 cm, and BWref=75.1 kg (Ghezelbash et al. 2016).

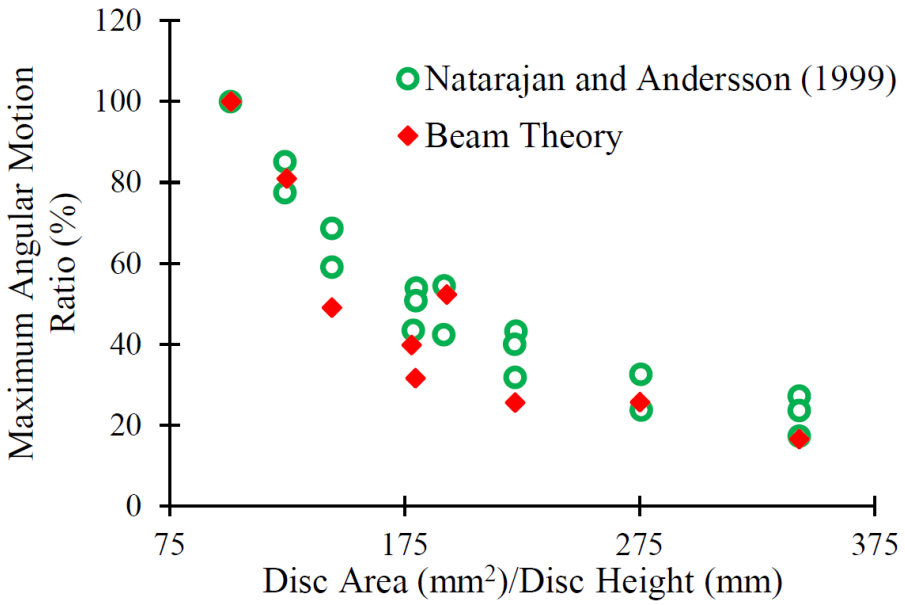

Fig. S2: Results of the beam theory against those of a finite element model of L3-L4 motion segment under 400 N compressive preload and 7.5 Nm moment (flexion, extension, lateral and axial) (Natarajan and Andersson 1999) for different values of disc height (5.5, 8.8 and 10.5 mm) and disc area (1060, 1512 and 1885 mm2).

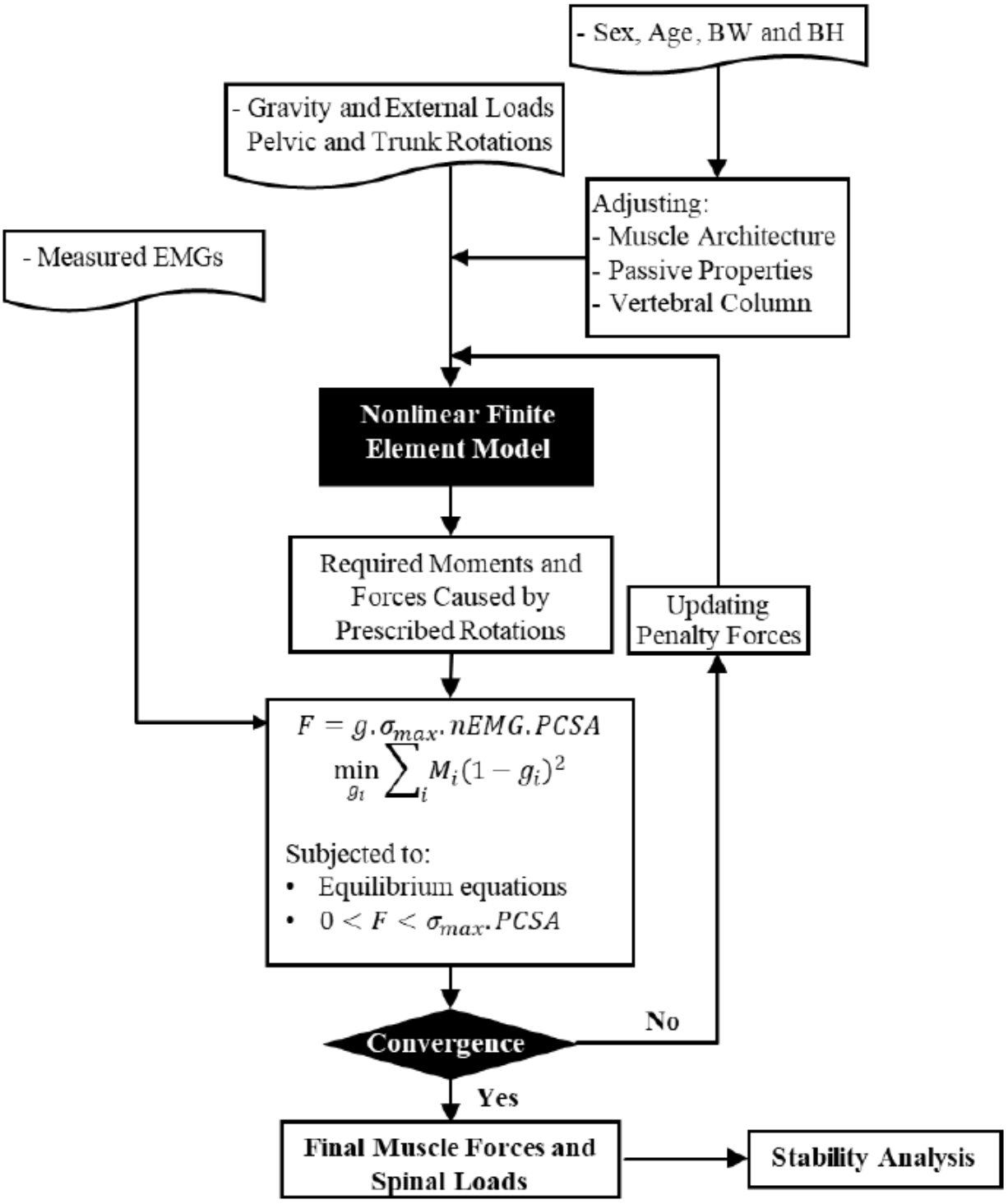

Fig. S3: The flowchart of the musculoskeletal model (BW: body weight; BH: body height).

References

Ghezelbash F, Shirazi-Adl A, Arjmand N, El-Ouaaid Z, Plamondon A Subject-specific biomechanics of trunk: musculoskeletal scaling, internal loads and intradiscal pressure estimation. Biomech Model Mechanobiol 2016; 15:1699-1712

Natarajan RN, Andersson GB The influence of lumbar disc height and cross-sectional area on the mechanical response of the disc to physiologic loading. Spine 1999; 24:1873